This article has been accepted for publication in a future issue of this journal, but has not been fully edited. Content may change prior to final publication. Citation information: DOI 10.1109/JSEN.2018.2857202, IEEE Sensors Journal

A low-power, low-noise 37-MHz photoreceiver for intersatellite laser interferometers using discrete heterojunction bipolar transistors

Germán Fernández Barranco*†, Benjamin S. Sheard*†‡, Christian Dahl *†§, Wolfgang Mathis, *Life Fellow, IEEE*¶ and Gerhard Heinzel*†

*Max Planck Institute for Gravitational Physics (Albert Einstein Institute), Callinstr. 38, 30167 Hanover, Germany

†Institut für Gravitationsphysik, Leibniz Universität Hannover, Callinstr. 38, 30167 Hanover, Germany

‡ EOS Space Systems Pty Limited, EOS House Mount Stromlo Observatory, Stromlo ACT 2611, Australia

§ SpaceTech GmbH (STI), Seelbachstrasse, 88090 Immenstaad am Bodensee, Germany

¶ Institut für Theoretische Elektrotechnik, Leibniz Universität Hannover, Appelstr. 9A, 30167 Hanover, Germany

***Abstract*—Intersatellite laser interferometers feature quadrant photoreceivers to produce electrical signals from the interfered optical beams. In the particular case of LISA, the expected optical AC beat note has an amplitude of the order of nW. This requires photoreceivers with an input current noise density of a few $\mathrm{pA\,Hz^{-1/2}}$ in each channel up to $25\,\mathrm{MHz}$. Additionally, the significant number of photoreceivers in a single spacecraft imposes tight constraints on the power consumption per device. We present the experimental characterization of a quadrant photoreceiver based on discrete heterojunction bipolar transistors and an off-the-shelf 0.5 mm diameter InGaAs quadrant photodiode, showing an input current noise density of $1.9\,\mathrm{pA\,Hz^{-1/2}}$ at $25\,\mathrm{MHz}$, a $3\,\mathrm{dB}$ bandwidth of $37\,\mathrm{MHz}$ and a total power consumption of $178\,\mathrm{mW}$.**

***Index Terms*—photoreceiver, transimpedance amplifier, heterodyne laser interferometry, intersatellite metrology, gravitational waves, geodesy.**

I. Introduction

Laser interferometry is a well-established technique to measure distance variations between test masses with unparalleled precision [1]. The future Laser Interferometer Space Antenna (LISA) will use this technology to detect gravitational waves in the $0.1\,\mathrm{mHz}$-$100\,\mathrm{mHz}$ frequency range [2]. Questions regarding the feasibility of LISA have been positively addressed by the LISA Pathfinder mission [3]. Additionally, the Laser Ranging Interferometer (LRI) of the GRACE-FO mission, with an expected launch in early 2018, will become the first laser interferometer between spacecraft [4]. Quadrant photoreceivers (QPRs) are crucial elements in the interferometer since they convert optical signals into electrical signals for further processing in the metrology chain. The particular conditions of an intersatellite laser interferometer impose demanding requirements on the QPRs. Particularly, the beat note obtained after interfering the local laser with the received, weak beam has an amplitude of the order of nW and a heterodyne frequency varying between $5\,\mathrm{MHz}$ and $25\,\mathrm{MHz}$ [2]. Therefore, QPRs with an input current noise of the order of a few $\mathrm{pA\,Hz^{-1/2}}$ within the MHz detection range are required. Furthermore, the QPR should separate the DC and AC (beat note) components of the resulting electrical signal. The complexity of the LISA metrology requires a significant number of QPRs in one single spacecraft to provide the necessary readout for the science, local and reference interferometers [2]. In addition to that, redundancy is desired in a space-based system, which also increases the number of QPR units. Consequently, the amount of QPRs limits the power consumption of each device.

The development of LISA-like quadrant photoreceivers has been focused on using custom-designed, low capacitance ($\sim 12.7\,\mathrm{pF\,mm^{-2}}$) indium gallium arsenide (InGaAs) quadrant photodiodes (QPDs) in combination with traditional operational-amplifier-only (OpAmp-only) transimpedance amplifiers (TIAs) [5]. Similarly, improvements in the noise performance of a MHz photoreceiver were achieved by lowering the effective capacitance of commercially available photodiodes via bootstrapping [6]. The latter option is not suitable for standard QPDs due to their common-cathode configuration. As opposed to previous methods, this work focuses on reducing the noise of the TIA electronics by combining discrete transistors with OpAmps. Last generation discrete transistors can outperform OpAmps commonly used in low noise TIA designs (see Section II). A discrete transistor, unlike OpAmps, allows the optimization of its noise parameters by adjusting its collector current I_C. The operating collector current, below a mA, also helps reducing the power consumption of the photoreceiver.

A particular type of discrete device, the silicon-germanium (SiGe) heterojunction bipolar transistor (HBT), has experienced an increase in popularity in the last decade due to its cost-effective production, whilst having similar performance to high-end semiconductor compounds such as gallium-arsenide (GaAs) [7] and indium phosphide (InP) [8].

We present a photoreceiver design for LISA based on heterojunction bipolar transistors (HBTs) and an off-the-shelf $0.5\,\mathrm{mm}$ InGaAs quadrant photodiode (QPD). The experimental characterization of this design shows an input current noise

Corresponding Author: german.fernandez.barranco@aei.mpg.de

This article has been accepted for publication in a future issue of this journal, but has not been fully edited. Content may change prior to final publication. Citation information: DOI 10.1109/JSEN.2018.2857202, IEEE Sensors Journal

of $1.9\,\mathrm{pA\,Hz^{-1/2}}$ at $25\,\mathrm{MHz}$, about $0.2\,\mathrm{pA\,Hz^{-1/2}}$ lower than a previous photoreceiver for LISA featuring the same QPD [9]. The reduction of photoreceiver electronic noise translates to a $0.13\,\mathrm{pm\,Hz^{-1/2}}$ reduction of the photoreceiver contribution to the LISA readout displacement noise. The interferometer displacement noise ultimately defines the observatory sensitivity to gravitational waves. The input current noise stays below $2\,\mathrm{pA\,Hz^{-1/2}}$ up to $30\,\mathrm{MHz}$, the same level obtained using custom-made low capacitance photodiodes in [5]. The $3\,\mathrm{dB}$ bandwidth of the developed photoreceiver is $37\,\mathrm{MHz}$. These results demonstrate that the implemented TIA exhibits the required bandwidth for LISA and lower noise than previous designs. Additionally, our design features different stages for the AC and DC components of the photocurrent, unlike the photoreceivers investigated in [5], [9]. The measured power consumption is $178\,\mathrm{mW}$, including all 4 DC and 4 AC channels. This power consumption is possible thanks to the transistor-based input stage and the OpAmps used, whose combined nominal quiescent current is below $5\,\mathrm{mA}$ per channel.

In Section 2, we present the structure of a generic QPR front-end, analyze the noise model of a bipolar transistor and discuss in detail the topology of the developed QPR based on HBTs. Section 3 contains the experimental characterization of the developed QPR. Finally, conclusions are provided in Section 4.

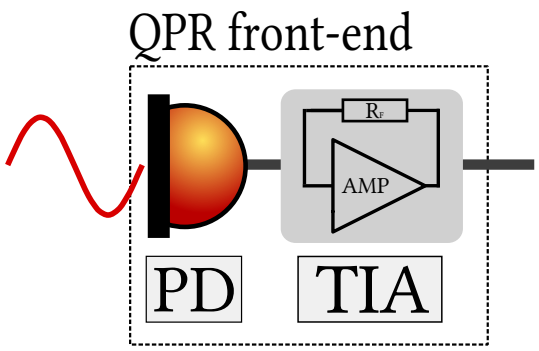

Fig. 1. Single channel block diagram of a quadrant photoreceiver (QPR) front-end, which is a combination of a quadrant photodiode (QPD) segment and a transimpedance amplifier (TIA). The QPR front-end is the most critical section regarding electronic noise and bandwidth.

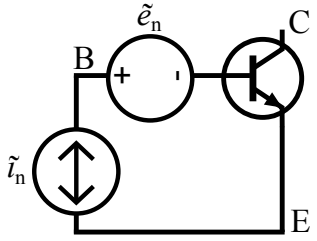

Fig. 2. Bipolar junction transistor (BJT) noise model. Similar to OpAmps, the noise of a BJT can be described with a voltage and a current noise source.

II. The QPR based on discrete transistors

The most critical section of the QPR regarding electronic noise [10] and bandwidth is the front-end. Figure 1 shows a block diagram of a single channel front-end. It comprises a QPD segment that converts the optical signal into current and the transimpedance amplifier (TIA), which converts current into voltage. In the standard OpAmp-based TIA, both the OpAmp current noise $\tilde{\imath}_\mathrm{n}$ and voltage noise $\tilde{e}_\mathrm{n}$ have been identified as key contributors to the QPR total input current noise density $\tilde{\imath}_\mathrm{T}$ in the $5\,\mathrm{MHz}$-$25\,\mathrm{MHz}$ LISA heterodyne frequency range [9]. So far, efforts have been focusing on using OpAmps with a good trade-off between $\tilde{\imath}_\mathrm{n}$ and $\tilde{e}_\mathrm{n}$, whilst, at the same time, reducing the junction capacitance of the QPD [5], which significantly increases $\tilde{\imath}_\mathrm{T}$ above $10\,\mathrm{MHz}$. Even though FET-based OpAmps commonly feature current noise $\tilde{\imath}_\mathrm{n}$ levels of the order of $\mathrm{fA\,Hz^{-1/2}}$, their significantly higher voltage noise $\tilde{e}_\mathrm{n}$ compared to their bipolar-based counterparts makes them unsuitable for the required noise levels in the MHz range. Many bipolar-based OpAmps in the market have remarkable noise properties, but the need for low $\tilde{\imath}_\mathrm{n}$, low $\tilde{e}_\mathrm{n}$ and low power consumption makes discrete bipolar junction transistors (BJTs) an attractive alternative for the TIA input stage.

Similar to OpAmps, the noise of a single transistor amplifier can be modeled with a voltage and a current noise source, as seen in Figure 2 [11]. The amount of noise generated by these two equivalent noise sources is determined not only by the physical properties of the device but also by its biasing. Equation 1 describes the voltage noise density $\tilde{e}_\mathrm{n}$ in a BJT.

$$\tilde{e}_\mathrm{n} = \sqrt{4kT\left(\frac{V_\mathrm{T}}{2I_\mathrm{C}} + r_{\mathrm{BB}'}\right)}, \qquad [\tilde{e}_\mathrm{n}] = \mathrm{V\,Hz^{-1/2}}, \tag{1}$$

where k is the Boltzmann constant, T the temperature, V_T the thermal voltage, I_C the transistor collector current and $\mathrm{r_{BB'}}$ its base spreading resistance. Equations 2 describes the current noise density $\tilde{\imath}_\mathrm{n}$ in a BJT at frequencies above the flicker-noise corner frequency and significantly lower than the transition frequency f_T, at which the small signal current gain equals one.

$$\tilde{\imath}_\mathrm{n} = \sqrt{2\mathrm{q}\frac{I_\mathrm{C}}{\beta_0}}, \qquad [\tilde{\imath}_\mathrm{n}] = \mathrm{A\,Hz^{-1/2}}, \tag{2}$$

where q is the charge of an electron and β_0 the current gain of the BJT at DC. The transistor parameters $\mathrm{r_{BB'}}$, β_0 and f_T are fixed by the BJT materials and its geometry, while I_C can be changed using different DC operating points. The use of discrete transistors in this work is motivated by the availability of last generation discrete BJTs with a base spreading resistance $\mathrm{r_{BB'}}$ of a few Ω, a current gain β_0 of several hundreds and a transition frequency f_T of tens of GHz. This type of discrete BJTs, placed at the input stage of the photoreceiver, have the potential to outperform bipolar-based OpAmps in terms of noise and bandwidth. Comparing Equations 1 and 2, we can observe a trade-off between $\tilde{e}_\mathrm{n}$ and $\tilde{\imath}_\mathrm{n}$ as a function of the collector current I_C. This type of optimization via I_C is not possible in integrated OpAmps. Additionally, the operating

This article has been accepted for publication in a future issue of this journal, but has not been fully edited. Content may change prior to final publication. Citation information: DOI 10.1109/JSEN.2018.2857202, IEEE Sensors Journal

collector current I_{C} of discrete transistors is in general lower than the quiescent current I_{Q} of the bipolar-based OpAmps adequate for LISA-like photoreceivers, translating to lower power consumption.

In the last decade, silicon-germanium (SiGe) HBTs have been improved to the point of being able to compete with traditional low noise technologies such as gallium-arsenide (GaAs) high electron mobility transistors (HEMTs) [7] and indium phosphide (InP) [8]. In particular, SiGe devices with a small percentage of carbon (SiGe:C) exhibit high f_{T} and low $\mathrm{r_{BB'}}$ values [12], which translate to high speed and low noise operation. The cost-effective nature of SiGe production favored the development of several generations of commercial discrete transistors based on this technology. The BFP842ESD, an HBT from Infineon Technologies based on SiGe:C and specifically designed for mobile communication low noise amplifiers, was chosen as the core element of a transistor-based TIA for a QPR design. The BFP842ESD was previously used in [13] to increase the signal-to-noise ratio (SNR) of a cryogenic pre-amplifier. By contrast, the input signals and environmental conditions of said study are drastically different compared to intersatellite laser interferometry. Using a theoretical estimation based on datasheet values and SPICE model parameters, the BFP842ESD has a voltage noise contribution $\tilde{e}_{\mathrm{n}} = 0.55\,\mathrm{nV\,Hz^{-1/2}}$ and a current noise contribution $\tilde{i}_{\mathrm{n}} = 1\,\mathrm{pA\,Hz^{-1/2}}$ at a collector current of $1\,\mathrm{mA}$. The emitter-base capacitance C_{EB}, which contributes to the amplifier input capacitance, is $0.44\,\mathrm{pF}$. On the other hand, SPICE models do not always reflect the noise of the device at the specific conditions of the desired circuit. Models of the same device from different manufacturers can also present different noise parameters [14]. Additionally, the nominal specifications of a given component can differ from those of the actual device, as seen in the characterization of a LISA-like photoreceiver [9]. The work presented here relies on experimental measurements of the photoreceiver performance.

Figure 3 shows the circuit diagram of the TIA for one QPR channel. The current source with a capacitor C_{PD} in parallel represents the electrical model of a QPD segment. The photocurrent produced by the reverse-biased QPD ($\mathrm{V_{bias}} = 5\,\mathrm{V}$) splits into an AC (science signal) and a DC path. The BFP842ESD is used in a common emitter configuration as the first stage of the AC signal path. The first stage is the most critical since the signal needs to be amplified without introducing excessive noise. The resistors used to adjust the base voltage of the BFP842ESD (R_1 and R_2) were intentionally chosen to exhibit a high resistance in order to reduce their Johnson current noise contribution. Another discrete HBT (BFR181) follows the BFP842ESD in a cascode configuration, reducing the Miller effect and maintaining a high bandwidth [11]. The amplification of the cascode is given by the DC current gain of the BFP842ESD, which for a $\sim 1\,\mathrm{mA}$ collector current is about 350 [15]. With this amplification at the first stage, the noise contribution from subsequent elements such as the resistor R_6 and the OpAmp N_1 is less critical [10]. An OpAmp-based non-inverting amplifier is used to obtain an additional voltage gain of 5. Since an outstanding noise performance is not necessary for this secondary stage, the

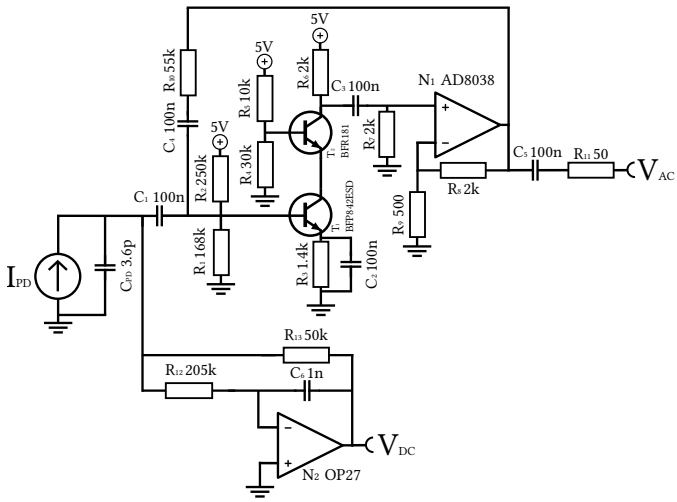

Fig. 3. Circuit diagram of the TIA for one QPR channel. The current source with a capacitance in parallel represents a QPD segment. The photocurrent splits into an AC and a DC path. The low noise heterojunction bipolar transistor (HBT) BFP842ESD is used in a common emitter configuration as the first stage of the AC path. R_1 and R_2 have intentionally high resistances to reduce their Johnson current noise contribution. A cascode structure and an additional low power non-inverting amplifier are used to maintain the bandwidth and increase the gain. The DC path features a standard OpAmp-based TIA (OP27).

AD8038 from Analog Devices was selected due to its low power consumption (Quiescent current $I_{\mathrm{Q}} = 1\,\mathrm{mA}$) and a 3 dB bandwidth of $350\,\mathrm{MHz}$ with unity gain. Stability and AC transimpedance gain are achieved by applying negative feedback from the AD8038 output to the BFP842ESD input (base).

For the DC path, a more standard OpAmp-based TIA is used to convert the DC component of the photocurrent, which is mainly produced by the local laser beam of the interferometer. Since MHz operation is not needed in this signal path, the common OP27 was selected. Aside from the feedback resistor R_{13}, a $200\,\mathrm{k\Omega}$ resistor is used to isolate the OP27 output from the sensitive input node. These two nodes would otherwise be connected at high frequencies, when C_6 takes on a low impedance.

The TIA supply voltage is $\pm 5\,\mathrm{V}$. The AC output voltage is not critical for the supply range. On the other hand, the DC output voltage is about $-4\,\mathrm{V}$ during nominal operation, therefore a supply range from $1\,\mathrm{V}$ to $-5\,\mathrm{V}$ is needed to provide enough margin. In our design, using $5\,\mathrm{V}$ instead of $1\,\mathrm{V}$ was a choice of convenience, since $5\,\mathrm{V}$ is also the bias voltage needed for the QPD. Although we have mainly focused on reducing the supply current to improve the power consumption of the photoreceiver, future designs could also benefit from a lower positive supply voltage. Noise from the power supply is in general not critical at the required MHz heterodyne band where photoreceiver electronic noise is measured. Additionally, bypass capacitors filter residual high frequency noise from the supply lines.

All four channels of the QPR feature the same values for all electronic components. The SMD resistors and capacitors used have a 1% and 10% tolerance, respectively. The QPR was built on a two-sided printed circuit board (PCB). The layout

This article has been accepted for publication in a future issue of this journal, but has not been fully edited. Content may change prior to final publication. Citation information: DOI 10.1109/JSEN.2018.2857202, IEEE Sensors Journal

follows standard radio-frequency (RF) design techniques. All components were placed on the bottom side, leaving the top layer of the PCB solely as a ground plane. Cutouts were performed on both sides of the PCB in areas surrounding the main signal path to avoid parasitic effects. Copper tracks were kept as short as possible to minimize unwanted delays. To avoid interruptions of the signal path or ground plane, the regulated $\pm 5\,\mathrm{V}$ from the power supply were distributed using copper wires with a cross-sectional area of $0.2\,\mathrm{mm}^2$. A set of $100\,\mathrm{nF}$ bypass capacitors were placed at the supply nodes not only to remove undesired supply noise but also to reduce the signal path to ground. Figure 4 is a picture of the bottom side of the populated PCB, where the QPD and all TIAs are visible.

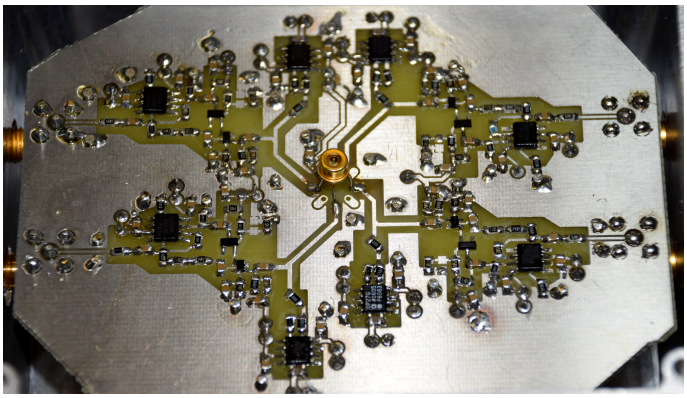

Fig. 4. Picture of the implemented QPR. The QPD (GAP500Q from OEC GmbH) and all TIAs (DC and AC) are visible on the bottom side of the PCB. The layout follows standard radio-frequency (RF) design techniques, including a dedicated ground plane, selective cutouts on sensitive areas, short copper tracks and bypass capacitors.

The QPD in Figure 4 is the GAP500Q from OEC GmbH, a $0.5\,\mathrm{mm}$ diameter InGaAs device. The measured junction capacitance (C_{PD}) of the GAP500Q sample used was $3.6\,\mathrm{pF}$ per segment. This capacitance is comparable to the C_{PD} = $2.5\,\mathrm{pF}$ of the $1\,\mathrm{mm}$ diameter InGaAs QPD developed by Discovery Semiconductors Inc and used in [5]. In general, larger area QPDs facilitate the alignment of components in an optical setup, but increase the noise and decrease the bandwidth of the QPR due to the larger junction capacitance.

Equation 3 describes the total input current noise $\tilde{\imath}_{\mathrm{en}}$ of the photoreceiver.

$$\tilde{\imath}_{\mathrm{en}} = \left(\tilde{\imath}_{\mathrm{J}}^2 + \tilde{\imath}_{\mathrm{DC}}^2 + \tilde{\imath}_{\mathrm{n}}^2 + \left(\frac{\tilde{e}_{\mathrm{n}}}{|Z_{\mathrm{T}}|}\right)^2\right)^{1/2}, \qquad (3)$$
$$[\tilde{\imath}_{\mathrm{en}}] = \mathrm{A\,Hz^{-1/2}},$$

where $\tilde{\imath}_{\mathrm{J}}$ is the Johnson current noise of the resistors at the input, $\tilde{\imath}_{\mathrm{DC}}$ is the residual current noise of the DC TIA and $|Z_{\mathrm{T}}|$ is the magnitude of the total impedance seen from the base of the input transistor (BFP842ESD). The impedance magnitude $|Z_{\mathrm{T}}|$ is inversely proportional to the frequency due to the presence of capacitances, which increases $\tilde{\imath}_{\mathrm{en}}$ towards high frequencies. A bigger photodiode junction capacitance C_{PD} magnifies this effect, which motivates the use of custom-made photodiodes with lower capacitance [5]. On the other hand, the use of HBTs as input transistors can mitigate this effect via lower voltage noise $\tilde{e}_{\mathrm{n}}$. The TIA gain over frequency G_{TIA} is given by Equation 4.

$$G_{\mathrm{TIA}} = \left|\frac{V_{\mathrm{o}}}{I_{\mathrm{i}}}\right| = \left|\frac{Z_{\mathrm{F}}}{\frac{1}{A_{\mathrm{OL}}\beta} + 1}\right|, \qquad (4)$$
$$[G_{\mathrm{TIA}}] = \Omega,$$

where Z_{F} is the feedback impedance, A_{OL} is the open-loop voltage gain and β is the transfer function of the feedback network [16]. The bandwidth of G_{TIA} depends on the transistor transition frequency f_{T}, which affects the open-loop voltage gain A_{OL}. It also depends on the photodiode junction capacitance C_{PD}, which influences the feedback network β.

III. Experimental Characterization of the QPR

In order to measure the QPR input current noise $\tilde{\imath}_{\mathrm{en}}$ and the transimpedance amplifier gain G_{TIA}, a shot-noise limited light source (halogen lamp) was used as described in [9]. The output voltage noise of the QPR is measured under different light levels, which allow us to derive both $\tilde{\imath}_{\mathrm{en}}$ and G_{TIA}. With our QPR design, the voltage noise is measured at the output of the AC path. The DC output and the DC photocurrent gain ($50\,\mathrm{k\Omega}$) are used to calculate the shot noise introduced by the halogen lamp. The device utilized to read out the voltage from the AC and the DC outputs was an Agilent Technologies MSO-X 4054A $5\,\mathrm{GS\,s^{-1}}$ oscilloscope. Once the data is digitized and transferred to a computer, the voltage noise spectral densities, obtained using the Welch's FFT method [17], are used together with the shot noise to calculate the input current noise density. Additionally, the gain of the TIA over frequency can be extracted in the process. All measurements have been performed at room temperature, which is essentially the real-life temperature of the device during operation.

Figure 5 shows the input current noise density $\tilde{\imath}_{\mathrm{en}}$ and the transimpedance amplifier gain G_{TIA} over frequency for one QPR channel. The measurement was repeated with different transistor collector currents (I_{C}). The higher noise towards high frequencies indicates that the input current noise $\tilde{\imath}_{\mathrm{en}}$ above $20\,\mathrm{MHz}$ is dominated by the TIA voltage noise $\tilde{e}_{\mathrm{n}}$ component (see Equation 3). The input current noise density $\tilde{\imath}_{\mathrm{en}}$ decreases with higher I_{C} at frequencies above $20\,\mathrm{MHz}$, indicating a decrease in the voltage noise $\tilde{e}_{\mathrm{n}}$ (as described by Equation 1). The bandwidth of G_{TIA} also improves with increasing I_{C}. This is likely produced by an increase of the transition frequency f_{T} at the input transistors [15], which increases the bandwidth of the open-loop voltage gain A_{OL} (Equation 4). The noise at $25\,\mathrm{MHz}$, which is the maximum heterodyne frequency expected in LISA, reaches a minimum at I_{C} = $0.75\,\mathrm{mA}$ and does not improve (nor deteriorate) with higher collector currents. Combining this quantitative experimental analysis with the expected BJT noise behavior (Equations 1 and 2), we can argue that the BFP842ESD base spreading resistance $r_{\mathrm{BB'}}$ could be limiting the input current noise density $\tilde{\imath}_{\mathrm{en}}$ of the photoreceiver.

Figure 6 presents the input current noise density and TIA gain over frequency of the four QPR channels at a collector

This article has been accepted for publication in a future issue of this journal, but has not been fully edited. Content may change prior to final publication. Citation information: DOI 10.1109/JSEN.2018.2857202, IEEE Sensors Journal

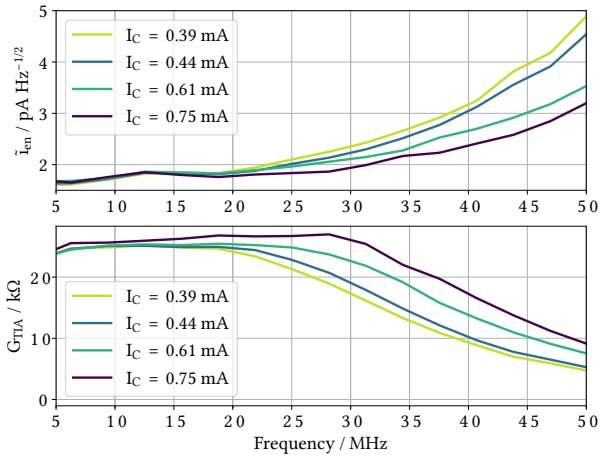

Fig. 5. Input current noise $\tilde{\imath}_{\mathrm{en}}$ and transimpedance gain G_{TIA} over frequency for one QPR channel. The measurement was repeated with different transistor collector currents (I_{C}). The input current noise density decreases with higher I_{C} at frequencies above 20 MHz. The bandwidth of the TIA also improves with increasing I_{C}. The noise at 25 MHz, which is the maximum heterodyne frequency expected in LISA, reaches a minimum at I_{C} = 0.75 mA. This limitation is probably caused by the transistor base spreading resistance $r_{\mathrm{BB'}}$.

current $I_{\mathrm{C}} = 0.75\,\mathrm{mA}$. All four channels exhibit a similar behavior, with an input current noise of $1.7\,\mathrm{pA\,Hz^{-1/2}}$ at 5 MHz, increasing to $1.9\,\mathrm{pA\,Hz^{-1/2}}$ at 25 MHz, the maximum heterodyne frequency in LISA. The input current noise stays below $2\,\mathrm{pA\,Hz^{-1/2}}$ up to 30 MHz. The 3 dB bandwidth of G_{TIA} is 37 MHz. In contrast to the design presented in this text, previous 4-channel LISA-like photoreceivers based on discrete transistors showed discrepancies in the performance among different channels [18]. The input-referred current noise of the photoreceiver, or photoreceiver electronic noise, is currently the second largest contribution in the LISA readout noise budget, after shot noise. During nominal operation, around 181 µW of optical power from the spacecraft's local laser arrive at each photodiode's segment, generating shot noise. The current noise density associated to shot noise is around $6.3\,\mathrm{pA\,Hz^{-1/2}}$, about 3.3 times higher than the photoreceiver electronic noise at 25 MHz in our design. The noise at 25 MHz is $0.2\,\mathrm{pA\,Hz^{-1/2}}$ below the noise measured in a previous LISA-like photoreceiver featuring the same QPD [9]. The reduction of photoreceiver noise translates to a $0.13\,\mathrm{pm\,Hz^{-1/2}}$ decrease of the contribution to the LISA readout displacement noise. The displacement noise is obtained using the equations in [19] and assuming the expected interferometer conditions of LISA, where a 181 µW beam from the local oscillator interferes with a weak received beam of about 30 pW on a photodiode's segment. The interferometer displacement noise ultimately defines the capability of the instrument to detect gravitational waves. The photoreceivers in [5], [9] use the ultra-low noise, high bandwidth EL5135 operational amplifier from Intersil as the core of the TIA. The EL5135 features a current noise density $\tilde{\imath}_{\mathrm{n}}$ of $0.9\,\mathrm{pA\,Hz^{-1/2}}$, a voltage noise density $\tilde{e}_{\mathrm{n}}$ of $1.5\,\mathrm{pV\,Hz^{-1/2}}$ and a gain bandwidth product of 1500 MHz. The results shown in Figure 6 and discussed above demonstrate that our TIA based on heterojunction bipolar transistors surpasses the noise performance of the EL5135. In comparison, the best commercially available photoreceivers to the knowledge of the authors, operating at the required wavelength and bandwidth (the 1811 from Newport [20]) features an input current noise of $2.5\,\mathrm{pA\,Hz^{-1/2}}$ at 10 MHz, which increases towards higher frequencies.

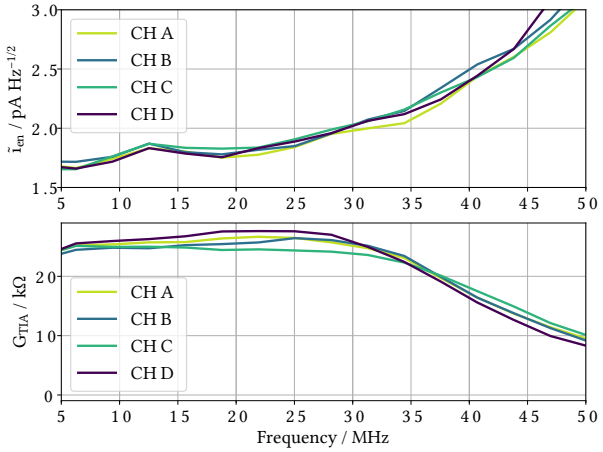

Fig. 6. Input current noise $\tilde{\imath}_{\mathrm{en}}$ and transimpedance gain G_{TIA} of the four QPR channels, using a collector current I_{C} of 0.75 mA. All four channels exhibit a similar behavior, with an input current noise of $1.7\,\mathrm{pA\,Hz^{-1/2}}$ at 5 MHz, increasing to $1.9\,\mathrm{pA\,Hz^{-1/2}}$ at 25 MHz, which is the maximum heterodyne frequency in LISA. The noise at 25 MHz is $0.2\,\mathrm{pA\,Hz^{-1/2}}$ below the noise measured in a previous LISA-like photoreceiver featuring the same QPD [9]. The noise stays below $2\,\mathrm{pA\,Hz^{-1/2}}$ up to 30 MHz. The 3 dB bandwidth of G_{TIA} is 37 MHz.

In order to study the impact of a lager photodiode junction capacitance on the transistor-based design, the GAP500Q was replaced by a 1 mm diameter InGaAs QPD: the GAP9119 from OEC GmbH (also called GAP1000Q). Figure 7 shows a comparison of the input current noise density and bandwidth of a QPR channel using both QPD models. The higher photodiode capacitance ($C_{\mathrm{PD}} = 11.5\,\mathrm{pF}$) magnifies the effect of the total impedance magnitude $|Z_{\mathrm{T}}|$ on the input current noise (see Equation 3). The input current noise stays below $3\,\mathrm{pA\,Hz^{-1/2}}$ at 25 MHz. The 3 dB bandwidth of G_{TIA} was determined to be 24 MHz. The higher photodiode capacitance reduces the G_{TIA} bandwidth due to its effect on the feedback network β (see Equation 4).

The power consumption of the QPR was measured using the current flowing through the ±5 V supply lines. The value obtained was 178 mW, with the OP27 from the DC path being the largest contributor (Quiescent current $I_{\mathrm{Q}} = 3\,\mathrm{mA}$). This power consumption is possible thanks to the transistor-based AC input stage and the low power operational amplifiers at the DC stage (OP27) and the second AC stage (AD8038). Low noise, high bandwidth operational amplifiers used in previous photoreceiver designs have relatively high quiescent currents. For instance, the EL5135 and the LMH6624, which could be used in an OpAmp-only AC stage, feature nominal quiescent currents of 6.7 mA and 11.4 mA respectively. In our design, the combination of the cascode current with the nominal AD8038 quiescent current stays below 2 mA.

This article has been accepted for publication in a future issue of this journal, but has not been fully edited. Content may change prior to final publication. Citation information: DOI 10.1109/JSEN.2018.2857202, IEEE Sensors Journal

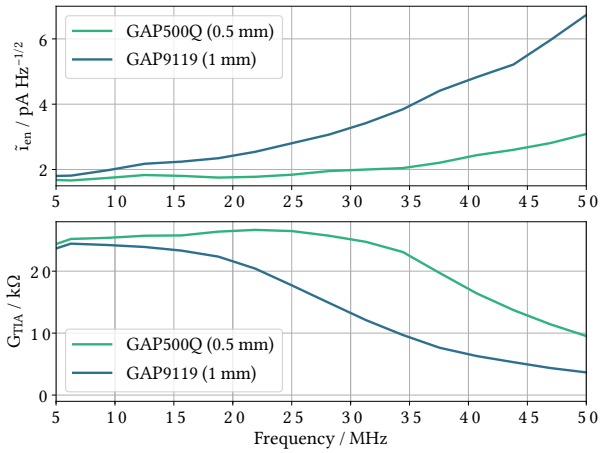

Fig. 7. Comparison of the input current noise $\tilde{i}_{\mathrm{en}}$ and transimpedance gain G_{TIA} of one QPR channel using a GAP500Q (C_{PD} = 3.6 pF) and a GAP9119/GAP1000Q (C_{PD} = 11.5 pF). The input current noise density using the GAP9119 is higher but stays below $3\,\mathrm{pA\,Hz^{-1/2}}$ at 25 MHz. The 3 dB bandwidth of G_{TIA} is 24 MHz.

IV. Conclusions

We have designed, implemented and characterized a new type of quadrant photoreceiver (QPR) front-end for intersatellite laser interferometry. The transimpedance amplifier (TIA) was optimized using a heterojunction bipolar transistor (HBT) designed for GHz mobile applications, the BFP842ESD from Infineon Technologies, as the input stage of the AC section. The QPR features a GAP500Q, a 0.5 mm diameter InGaAs quadrant photodiode (QPD) with a junction capacitance of 3.6 pF per segment. All four channels exhibit an input current noise of $1.9\,\mathrm{pA\,Hz^{-1/2}}$ at the LISA maximum heterodyne frequency, 25 MHz. The measured noise is $0.2\,\mathrm{pA\,Hz^{-1/2}}$ below the noise obtained in a previous design based on the EL5135 operational amplifier and the same QPD. The reduction of photoreceiver noise translates to a $0.13\,\mathrm{pm\,Hz^{-1/2}}$ reduction of the QPR contribution to the LISA readout displacement noise. The interferometer displacement noise in LISA ultimately defines its sensitivity detecting gravitational waves. The input current noise stays below $2\,\mathrm{pA\,Hz^{-1/2}}$ up to 30 MHz. The 3 dB bandwidth was measured to be 37 MHz. The effect of the collector current of the input transistor on the noise and bandwidth was studied. The collector current represents an adjustable design parameter not available in traditional OpAmp-only TIAs. An additional characterization using a larger QPD (GAP9119/GAP1000Q), which has a greater junction capacitance per segment (C_{PD} = 11.5 pF), shows an input current noise density below $3\,\mathrm{pA\,Hz^{-1/2}}$ at 25 MHz and a 3 dB bandwidth of 24 MHz. The measured power consumption of the full QPR front-end is 178 mW, thanks to the low power, transistor-based input stage and the OpAmps used (OP27 and AD8036). This constitutes an improvement compared to standard OpAmp-only photoreceiver designs. This new type of QPR front-end represents a good alternative to traditional OpAmp-based designs for future intersatellite interferometry missions due to its low noise, high bandwidth, and low power consumption.

Acknowledgments

The authors acknowledge the funding provided the Bundesministerium für Bildung und Forschung (BMBF) (03F0654B) and the International Max Planck Research School on Gravitational Waves (IMPRS-GW). The authors would also like to thank Nikolai Beev for the fruitful discussions about low noise heterojunction bipolar transistors.

References

[1] LIGO Scientific Collaboration and Virgo Collaboration. "GW150914: The Advanced LIGO detectors in the era of first discoveries". *Physical review letters*, 116(13):131103, 2016.

[2] M. Armano, H. Audley, P. Binetruy, M. Born, *et al.,* "Laser Interferometer Space Antenna". *arXiv preprint arXiv:1702.00786*, 2017.

[3] M. Armano, H. Audley, G. Auger, J. T. Baird *et al.*, "Sub-Femto-*g* Free Fall for Space-Based Gravitational Wave Observatories: LISA Pathfinder Results". *Phys. Rev. Lett.*, 116:231101, Jun 2016.

[4] B.S. Sheard, G. Heinzel, K. Danzmann, D.A. Shaddock, W.M. Klipstein, and W.M. Folkner. "Intersatellite laser ranging instrument for the GRACE follow-on mission". *Journal of Geodesy*, 86(12):1083–1095, 2012.

[5] A. Joshi, S. Datta, J. Rue, J. Livas, R. Silverberg, and Felipe Guzman Cervantes. "Ultra-low noise large-area InGaAs quad photoreceiver with low crosstalk for laser interferometry space antenna", 2012.

[6] H. Zhou, W. Wang, C. Chen, and Y. Zheng. "A Low-Noise, Large-Dynamic-Range-Enhanced Amplifier Based on JFET buffering input and JFET bootstrap structure". *IEEE Sensors Journal*, 15(4):2101–2105, 2015.

[7] J.C. Bardin. "Silicon-Germanium heterojunction bipolar transistors for extremely low-noise applications". Ph.D. thesis, California Institute of Technology, 2009.

[8] S. P. Voinigescu, T. O. Dickson, R. Beerkens, I. Khalid and P. Westergaard. "A comparison of Si CMOS, SiGe BiCMOS, and InP HBT technologies for high-speed and millimeter-wave ICs". *IEEE Topical Meeting on Silicon Monolithic Integrated Circuits in RF Systems. Digest of Papers*, pp. 111–114, 2004.

[9] F. Guzmán Cervantes, J. Livas, R. Silverberg, E. Buchanan, and R. Stebbins. "Characterization of photoreceivers for LISA". *Classical and Quantum Gravity*, 28(9):094010, 2011.

[10] H.T. Friis. "Noise figures of radio receivers". *Proceedings of the IRE*, 32(7):419–422, 1944.

[11] P. Horowitz and W. Hill. "The Art of Electronics" (Cambridge University, 2015), 3rd edition.

[12] J.D. Cressler. "Silicon Heterostructure Handbook: Materials, Fabrication, Devices, Circuits and Applications of SiGe and Si Strained-Layer Epitaxy" (CRC, 2005).

[13] M.J. Curry, T.D. England, N.C. Bishop, G. Ten-Eyck, J.R. Wendt, T. Pluym, M.P. Lilly, S.M. Carr, and M.S. Carroll. "Cryogenic preamplification of a single-electron-transistor using a silicon-germanium heterojunction-bipolar-transistor". *Applied Physics Letters*, 106(20):203505, 2015.

[14] V. Janásek, "Design of ultra low noise amplifiers," April, 2018. [Online]. Available: http://www.janascard.cz/aj_Download.html [Accessed Jun. 11, 2018].

[15] Infineon Technologies AG, "BFP842ESD. Robust Low Noise Silicon Germanium Bipolar RF Transistor," April, 2013 [Online]. Available: https://www.infineon.com/dgdl/Infineon-BFP842ESD-DS-v01_01-en.pdf?fileId=db3a3043394427e401394df03a3a27c9. [Accessed Jun. 11, 2018]

[16] X. Ramus, "Transimpedance Considerations for High-Speed Amplifiers," November, 2009 [Online]. Available: http://www.ti.com/lit/an/sboa122/sboa122.pdf. [Accessed Jun. 11, 2018].

[17] P. Welch. "The use of fast Fourier transform for the estimation of power spectra: a method based on time averaging over short, modified periodograms". *IEEE Transactions on audio and electroacoustics*, 15(2):70–73, 1967.

[18] C. Dahl. "Development of core elements for the LISA optical bench - Electro-optical measurement systems and test devices". Ph.D. thesis, Leibniz Universität Hannover, 2013.

[19] G. Fernández Barranco, O. Gerberding, T. S. Schwarze, B. S. Sheard, C. Dahl, B. Zender, and G. Heinzel. "Phase stability of photoreceivers in intersatellite laser interferometers". *Opt. Express*, vol. 25, no. 7, pp. 7999–8010, 2017.

[20] Newport, "Optical Receiver, 900-1700 nm InGaAs Detector, 25 kHz - 125 MHz Bandwidth," 2012 [Online]. Available: https://www.newport.com/medias/sys_master/images/images/h24/h48/8796989259806/18X1-125MHz-RCVR-180413J.pdf. [Accessed Jun. 11, 2018]